IEEE Access
Multidisciplinary ⋮ Rapid Review ⋮ Open Access Journal

Received July 27, 2018, accepted September 7, 2018, date of publication September 24, 2018, date of current version December 3, 2018.

Digital Object Identifier 10.1109/ACCESS.2018.2872062

Optimal Sliding Mode Controller Design Based on Dynamic Differential Evolutionary Algorithm for Under-Actuated Crane Systems

ZHE SUN[1], XUEJIAN ZHAO[1], ZHIXIN SUN[1], FENG XIANG[2], AND CHUNJING MAO[2]

[1]Key Laboratory of Broadband Wireless Communication and Sensor Network Technology, Nanjing University of Posts and Telecommunications, Nanjing 210023, China

[2]National Engineering Laboratory for Logistics Information Technology Sharing and Application, Yuantong Express Co., Ltd., Shanghai 201705, China

Corresponding author: Zhixin Sun (sunzx@njupt.edu.cn)

This work was supported in part by the Natural Science Foundation of Jiangsu Province under Grants BK20160913 and BK20140883, in part by the High Level Teacher Research Foundation of the Nanjing University of Posts and Telecommunications under Grant NY2016021, in part by the Chinese Natural Science Incubation Foundation of the Nanjing University of Posts and Telecommunications under Grant NY217055, in part by the Jiangsu Postdoctoral Foundation under Grant 1701016A, in part by the Natural Science Foundation of China under Grants 61602259, 61373135, and 61672299, and in part by the National Engineering Laboratory for Logistics Information Technology Sharing and Application of Yuantong Express Co., Ltd.

ABSTRACT In this paper, aiming at the payload residual vibration problem, a dynamic differential evolutionary algorithm-based sliding-mode controller (DDE-SMC) is designed for the under-actuated crane systems. According to the under-actuated crane systems mechanism of action, a fusion sliding function combined with position and angle sliding function is first given, and the corresponding control law by incorporating switching and equivalent control law is designed during the control process. Moreover, in order to configure the control parameter efficiently, the DDE algorithm is proposed and utilized for improving the anti-swing control performance. Through computer simulation and comparisons under different operation conditions, the proposed DDE-SMC demonstrates the effectiveness in damping the payload oscillations of the under-actuated crane system.

INDEX TERMS Dynamic DE algorithm, sliding mode controller, parameter optimization, under-actuated crane.

I. INTRODUCTION

As one of the most important transportation facility, under-actuated cranes are widely applied in harbors, construction site and industrial factories for the heavy cargoes transportation. According to the structural difference, under-actuated crane can be classified overhead crane, boom crane and tower crane. Among these kinds of cranes, overhead crane is the most representative and commonly used crane. According to the overhead crane operation feature, the trolley should carry the payload rapidly and do not cause any excessive movement at the appointed position. Besides, the swing of the payload should keep small as possible for avoiding the unnecessary collision or accident. But the high speed trolley movement easily causes payload swing in large amplitude so as to give rise to the potential safety hazard. Meanwhile, the under-actuated crane is a kind of typical under-actuated system, i.e., the degrees of freedom are more than the independent control inputs, which this intrinsic characteristic brings enormous challenges in anti-swing control. Hence, it is significant to design anti-swing controller for overhead crane.

Over the last decades, extensive researches have been studied for the anti-swing control of under-actuated cranes. At the early research stage, the input shaping [1], [2] and optimal control [3] have widely used for overhead cranes anti-swing control to reduce the residual vibration owing to the advantages of the easy designing difficulty and low hardware cost. However, the control performance might be degraded badly when the model parameter are inaccurate. In order to solve the adverse effect from the tiny variation of system parameter or external disturbances, various close-loop feedback control methods are gradually developed to make

up for the deficiency of open-loop control. In [4] and [5], researchers adopt PID control method and dual-state observer method for suppressing vibrations. The linear control method can better adapt to the change of system parameters, and has the merits of simple structure and easy design. However, this kind of method is based on the linearized model, which inevitably ignored the nonlinear characteristics of the overhead crane, and thereby leading to an unsatisfied anti-swing control performance in actual overhead crane control. For figuring out the nonlinear characteristic of overhead crane, numerous nonlinear control methods [6]–[9] are proposed for overhead crane systems. Generally, the aforementioned nonlinear control methods fully consider the nonlinear and under-actuated characteristic of the overhead crane, and make the control performance has a lot of ascension in oscillation elimination aspect.

Sliding mode control [10]–[19] is a commonly used variable structure control scheme owing to the merits of the simplicity and robustness against disturbances. Such as, Ngo and Hong [11] developed a sliding mode anti sway control method for offshore container crane. By designing the sliding surface and incorporating the trolley dynamics, the sway of payload has been damped effectively. Researchers proposed a self-adaptive sliding mode controller for crane system when the priori knowledge of the payload mass and damped elements are unknown [11]. An integral sliding mode controller is designed for overhead crane systems, and suboptimal integral sliding mode is determined by using the proposed extended Theta-D method [12]. In [13], for vanishing oscillation of overhead crane, researchers proposed a novel non-linear control scheme by incorporating the partial feedback linearization and sliding mode technique for the cargo anti-swing control and trolley tracking control. In order to cope with system uncertainties, a fuzzy logic uncertainty observer based sliding-mode anti-swing control law was developed for overhead crane [14]. Pezeshki *et al.* [16] proposed a Sugeno fuzzy algorithm based sliding mode controller for coping with the overhead crane dynamic characteristic.

To configure the control parameters and mode parameters are vitally important for eliminating the chattering and improving robustness. However, the conventional search algorithm such as gradient decent algorithm, Levenberg-Marquart algorithm, genetic algorithm, etc are easily trap into local optima for those complex parameter optimization problem. Hence, it is significant to adopt a powerful evolutionary algorithm for solving the parameter configuration problem. Comparing with other heuristic evolutionary algorithms, differential evolution (DE) algorithm is a certified and efficient optimizing algorithm and has been widely and successfully applied to various engineering optimization fields due to its excellent global search efficiency [20]–[28]. However, the search performance is easily affected due to the parametric sensitivity problem. Therefore, aiming at this problem, a dynamic scaling factor which is inspired by genetic scheme is introduced for enhancing the global search performance, and the improved DE algorithm is adopted to the sliding mode controller optimization process to strengthen the anti-swing control performance.

This paper is organized as follows. The brief description of overhead crane is stated in Section 2; Section 3 states the dynamic DE algorithm; The sliding mode controller and parameter optimization is addressed in Section 4; The experimental simulation results and comparisons are discussed in Section 5; The conclusions are summarized in the final section of this paper.

II. THE DESCRIPTION OF OVERHEAD CRANE SYSTEMS

Overhead crane systems is regarded as a nonlinear dynamic systems, and the intrinsic under-actuated characteristic also give rise to the difficulties for damping payload oscillation. As show in Fig.1, the overhead crane systems is composed of trolley and payload subsystems. Note that, the trolley will move at the horizontal direction by the driving force, and then, the payload will swing along with the trolley movement. In order understand the dynamic characteristic of overhead crane systems easily, we assume that the rope is inflexible and the rope weight is not consider, the payload swing along with x-y surface, and the friction between trolley and rail is ignored.

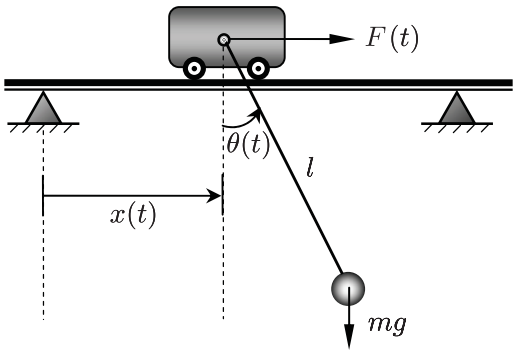

FIGURE 1. Two dimension overhead crane systems.

By adopting Lagrangian method, the corresponding equation of the generalized coordinate q_i is described as

$$\frac{d}{dt}\left(\frac{\partial La}{\partial \dot{q}_i}\right) - \frac{\partial La}{\partial q_i} = T_i \tag{1}$$

where $i = 1, 2$, $La = K - P$ (K and P represent the system kinetic energy and potential energy respectively.), q_i denotes the generalized coordination.(q_1 and q_2 are x and θ, respectively), and T_i is the external applied force.

Here, we assume that the payload is considered as a material particle, then, the system kinetic energy is acquired as follows

$$K = \frac{1}{2}M\dot{x}^2 + \frac{1}{2}mv^2 \tag{2}$$

where v is a vector and it denotes the payload velocity, defined as

$$v^2 = v_x^2 + v_y^2 \tag{3}$$

where $v_x = \dot{x} + l\dot{\theta}cos\theta$ and $v_y = -l\dot{\theta}sin\theta$. Here, we assume the payload as a particle, then the moment of inertia can be ignore in equation (2).

As shown in Fig.1, the system potential energy can be expressed by the potential energy of the payload subsystem because the potential energy of the trolley subsystem is invariable. The corresponding expression is depicted as

$$P = mgl(1 - cos\theta) \tag{4}$$

where g represents the gravitational acceleration. According to the equation (2) and equation (4), La is described as

$$La = K - P = \frac{1}{2}M\dot{x}^2 + \frac{1}{2}mv^2 - mgl(1 - cos\theta) \tag{5}$$

Considering the partial differential La as for x and letting

$$\frac{\partial La}{\partial x} = 0 \tag{6}$$

Partial differential La with regard to $\dot{x}$ in equation (5) lets

$$\frac{\partial La}{\partial \dot{x}} = M\dot{x} + m(\dot{x} + l\dot{\theta}cos\theta) \tag{7}$$

Further, differentiating (7) for time t, the corresponding expression is depicted as

$$\frac{d}{dt}(\frac{\partial La}{\partial \dot{x}}) = M\ddot{x} + m(\ddot{x} + l\ddot{\theta}cos\theta - l\dot{\theta}^2 sin\theta) \tag{8}$$

The final Lagrangian expression as for the x can be stated as

$$\frac{d}{dt}(\frac{\partial La}{\partial \dot{x}}) - \frac{\partial La}{\partial x} = (m + M)\ddot{x} + ml(\ddot{\theta}cos\theta - \dot{\theta}^2 sin\theta) = F \tag{9}$$

Considering the partial differential La as for θ in equation (5) and letting

$$\begin{aligned}\frac{\partial La}{\partial \theta} &= m[(\dot{x} + l\dot{\theta}cos\theta)(-l\dot{\theta}sin\theta) + (l\dot{\theta}sin\theta)(l\dot{\theta}cos\theta)] \\ &\quad -mglsin\theta \\ &= -ml\dot{x}\dot{\theta}sin\theta - mglsin\theta\end{aligned} \tag{10}$$

Differentiating La for $\dot{\theta}$ in (5) yields

$$\begin{aligned}\frac{\partial La}{\partial \dot{\theta}} &= m[(\dot{x} + l\dot{\theta}cos\theta)(lcos\theta) + (-l\dot{\theta}sin\theta)(-l\dot{\theta}sin\theta)] \\ &= ml\dot{x}cos\theta + ml^2\dot{\theta}\end{aligned} \tag{11}$$

Further, differentiating the equation (11) as for time t, the form is described as

$$\frac{d}{dt}(\frac{\partial La}{\partial \dot{\theta}}) = ml\ddot{x}cos\theta - ml\dot{x}\dot{\theta}sin\theta + ml^2\ddot{\theta} \tag{12}$$

The final Lagrangian expression as for the θ can be stated as

$$\frac{d}{dt}(\frac{\partial La}{\partial \dot{\theta}}) - \frac{\partial La}{\partial \theta} = ml\ddot{x}cos\theta + ml^2\ddot{\theta} + mglsin\theta = 0 \tag{13}$$

From equation (9) and equation (13), the mechanism model of overhead crane systems for x and θ is acquired as follows

$$(M + m)\ddot{x} + ml(\ddot{\theta}\cos\theta - \dot{\theta}^2 \sin\theta) = F \tag{14}$$

$$\cos\theta + l\ddot{\theta} + g\sin\theta = 0 \tag{15}$$

Here, θ and x represent swing angle and the displacement respectively; m and M are denoted as payload and trolley mass respectively, l is the length of rope; F denotes the driving force.

Finally, the corresponding state space model expression can be described as

$$\begin{cases}\dot{x_1} = x_2 \\ \dot{x_2} = f_1(x) + g_1(x)u \\ \dot{x_3} = x_4 \\ \dot{x_4} = f_2(x) + g_2(x)u\end{cases} \tag{16}$$

where, $x = [x_1, x_2, x_3, x_4]^T$, $x_1 = x, x_3 = \theta$, x_2 and x_4 are respectively denoted as trolley and payload angular velocity; u is the driving force coming from controller; f_1, f_2, g_1 and g_2 are described as

$$f_1(x) = \frac{mlx_4^2 sinx_3 + mgsinx_3 cosx_3}{M + msin^2 x_3} \tag{17}$$

$$g_1(x) = \frac{1}{M + msin^2 x_3} \tag{18}$$

$$f_2(x) = \frac{(M + m)gsinx_3 + mlx_4^2 sinx_3 cosx_3}{(M + msin^2 x_3)l} \tag{19}$$

$$g_1(x) = \frac{cosx_3}{(M + msin^2 x_3)l} \tag{20}$$

III. DYNAMIC DIFFERENTIAL EVOLUTION ALGORITHM

As one of the heuristic algorithm, differential evolution algorithm has been widely various practical applications for systems optimization, parameter identification, scheduling solving and so on. Firstly, DE algorithm randomly generated NP individuals $x = \{x_1, x_2, \ldots, x_{NP}\}$ at start stage. Thereinto, the ith potential solution is denoted by the D-dimensional vector $x_i = [x_{i,1}, x_{i,2}, \ldots, x_{i,D}]$. In order to improve the dynamic performance, a dynamic scaling factor is designed for overcoming the parameter sensitivity of DE algorithm and improving the search efficiency.

A. MUTATION

There are three individuals $x_{r1}, x_{r2}, x_{r3} (x_{r1} \neq x_{r2} \neq x_{r3})$ need to be picked out at random. And these selected objective vectors must unconformity. The new mutant individual is produced based on the formula.

$$v_i = x_1 + F_m \cdot (x_2 - x_3) \tag{21}$$

where F_m is denoted as scaling parameter which controls the amplification of v_i, $(i \neq j = 1, 2, \ldots, NP)$. The value of the factor F_m plays an important role in optimization process. If we assign a big value to F_m, that means, it will have more opportunities to jump out the local optimal, but it also may cause to badly global convergence performance. Similarly, the small value for it has, the local search performance will be improve, but the premature convergence also will be appeared.

According to the genetic strategy, the dynamic scaling factor is adopted in different evolution stages for getting better

convergence performance. The dynamic value of F_{dm} can be calculated based on the formula as follows.

$$F_{dm} = \begin{cases} F_m^{ini}; & g \le a \\ F_m^{ini} - 2 * (\frac{g-a}{b-a})^2; & a \le g \le \frac{a+b}{2} \\ F_m^{ini} + 2 * (\frac{g-a}{b-a})^2 - 1; & \frac{a+b}{2} \le g \le b \\ F_m^{ini} - 1 & g \le b \end{cases} \quad (22)$$

where F_m^{ini} is the initial scaling factor, a and b are the adjustable coefficient, g is defined as current iteration number.

B. CROSSOVER

After finishing the differential mutation operation, DE algorithm then carry out the crossover operation to improve the diversity of population. The new individual $u_i = [u_{i,1}, u_{i,2}, \ldots, u_{i,D}]$ is created to mate the mutated individual v_i with x_i by using the following formula.

$$u_{i,j} = \begin{cases} v_{i,j}; & if\ (rand_j \le p_c) or j = rand_D \\ x_{i,j}; & if\ (rand_j > p_c) or j \ne rand_D \end{cases} \quad (23)$$

where $rand_j$ denotes the jth arbitrary number between 0 and 1. $p_c \in [0, 1]$ is a constant crossover probability. The $rand_D \in [1, D]$ ensure the $v_{i,j}$ element be obtained.

C. SELECTION

In order to determine the target or the trial vector which can survive to the next generation, in this section, we adopt greedy selection strategy to pick out the new individual from u_i and x_i. if the cost function value of u_i is superior to the x_i, the u_i will be selected, otherwise, the target individual x_i is reserved. Given minimum optimization problem $minf(x)$, the select operation is expressed as follows:

$$x_i^{t+1} = \begin{cases} u_i; & f(u_i) < f(x_i^t) \\ x_i^t; & f(u_i) \ge f(x_i^t) \end{cases} \quad (24)$$

D. NUMERICAL TEST

In this section, shown in TABLE 1, nine typical benchmark functions, namely Rosenbrock, Sphere, Hyper Ellipsoid, Schwefel ridge, Griewank, Ackley, Rastrigin, Schwefel, Salomon, are utilized to confirm the effectiveness of the proposed algorithm. The first four functions (f_1-f_4) are typical unconstrained uni-modal function. The rest of five test functions are commonly used unconstrained multi-modal function with large search space, numerous local optimum and fraudulence. All of test functions are simulated for high dimensional search space ($D = 30$). The standard genetic algorithm (GA), particle swarm optimization (PSO) and DE algorithm are respectively tested for demonstrating the validity of improved DE algorithm. The parameter configuration are listed in TABLE 2. And to be fair, every mentioned algorithm implement thirty times for each test function.

TABLE 1. Benchmark test function.

Formula	Range
$f_1(\mathbf{x}) = \sum_{i=1}^{D-1} 100(x_{i+1} - x_i^2)^2 + (1 - x_i)^2$	$[-30, 30]$
$f_2(\mathbf{x}) = \sum_{i=1}^{D} x_i^2$	$[-100, 100]$
$f_3(\mathbf{x}) = \sum_{i=1}^{D} 2^i * x_i^2$	$[-100, 100]$
$f_4(\mathbf{x}) = \sum_{k=1}^{D} (\sum_{i=1}^{k} x_i)^2$	$[-100, 100]$
$f_5(\mathbf{x}) = \frac{1}{4000} \sum_{i=1}^{D} x_i^2 - \prod_{i=1}^{D} \cos(\frac{x_i}{\sqrt{i}}) + 1$	$[-600, 600]$
$f_6(\mathbf{x}) = -20 \exp(-0.2\sqrt{\frac{1}{D} \sum_{i=1}^{D} x_i^2})$ $- \exp(\frac{1}{D} \sum_{i=1}^{D} \cos(2\pi x_i)) + 20 + e$	$[-30, 30]$
$f_7(\mathbf{x}) = \sum_{i=1}^{D} (x_i^2 - 10\cos(2\pi x_i) + 10)$	$[-5.12, 5.12]$
$f_8(\mathbf{x}) = 418.9829D + \sum_{i=1}^{D} [-x_i sin(\sqrt{\lvert x_i \rvert})]$	$[-500, 500]$
$f_9(\mathbf{x}) = -cos(2\pi * \sqrt{\sum_{i=1}^{D} x_i^2}) + 0.1 * \sqrt{\sum_{i=1}^{D} x_i^2} + 1$	$[-100, 100]$

TABLE 2. Parameter setting of GA, PSO,DE and DDE.

GA	PSO	DE	DDE
$G = 1000$	$G = 1000$	$G = 1000$	$G = 1000$
$NP = 50$	$NP = 50$	$NP = 50$	$NP = 50$
$p_{c1} = 0.6$	$c_1 = 2, c_2 = 2$	$p_c = 0.5$	$p_c = 0.5$
$p_m = 0.01$	$w_1 = 0.9$ $w_2 = 0.4$	$F_m = 0.6$	$F_m^{ini} = 1.2$
-	-	-	$a = 100$
-	-	-	$b = 950$

If the inequality $|O_b - O^*| \le \varepsilon = 10^{-10}$ is satisfied, then the optimization process will be ended. Here O_b represents the final optimized value by using optimizing algorithm, O^* represents the intrinsic optimal value, and ε is the precision requirement. The F_w, F_b and F_{av} represent the worst, best, average objective function value respectively, the $Iter_{av}$ is the average iteration number. The final average results are summarized in TABLE 3.

For the uni-modal functions ($f_1 \sim f_4$), comparing with standard GA, PSO and DE algorithm, the dynamic DE algorithm gives better results in convergent accuracy. In f_2 and f_3 functions testing, dynamic DE algorithm can satisfy the testing terminated condition in limited iteration. For f_1 and f_4 functions, dynamic DE algorithm still exhibits good results in convergence accuracy.

For the multi-modal functions ($f_5 \sim f_9$), it is obvious that the better optimal value are acquired by dynamic DE algorithm. For f_5, f_6, f_7, f_8, and f_9 functions, the dynamic DE algorithm shows better convergent performance. Interestingly, in function f_7 testing, standard DE algorithm acquired the worse optimized results to compare with GA and PSO. The main reason is the fixed algorithm parameters lead to the standard DE algorithm tramped into local optimal in some more complex optimizing problems. Through various benchmark functions testing, the dynamic DE algorithm exhibits

TABLE 3. Test results of benchmark function.

Functions		*GA*	*PSO*	*DE*	*DDE*
f_1	F_w	2.402e+3	1.279e+3	4.815e+1	2.771e+1
	F_b	3.592e+1	5.553e+1	2.833e+1	2.639e+1
	F_{av}	5.547e+2	3.879e+2	3.358e+1	2.700e+1
f_2	F_w	7.629e-1	5.469e-0	1.741e-4	5.1847e-7
	F_b	4.196e-1	2.724e-1	2.905e-5	6.6545e-8
	F_{av}	6.078e-1	1.054e-0	8.422e-5	1.5811e-7
f_3	F_w	8.064e+7	1.451e+5	1.863e-0	5.401e-4
	F_b	3.764e+6	9.129e+3	5.063e-1	1.497e-4
	F_{av}	3.782e+7	4.105e+4	1.095e-0	3.345e-4
f_4	F_w	1.166e+4	2.626e+3	3.791e+4	1.257e+3
	F_b	2.043e+3	8.917e+2	2.428e+4	6.461e+2
	F_{av}	6.565e+3	1.127e+3	3.052e+4	9.607e+2
f_5	F_w	1.032e-0	1.057e-0	1.757e-1	1.896e-6
	F_w	7.485e-1	2.977e-1	2.228e-4	2.148e-7
	F_{av}	9.516e-1	8.252e-1	1.158e-2	6.001e-7
f_6	F_w	4.415e-0	1.937e-0	3.891e-3	4.644e-4
	F_b	1.197e-0	1.149e-1	1.222e-3	1.095e-4
	F_{av}	2.526e-0	5.892e-1	2.446e-3	2.203e-4
f_7	F_w	8.516e+1	8.080e+1	1.721e+2	7.874e+1
	F_b	4.246e+1	2.538e+1	1.206e+2	5.747e+1
	F_{av}	5.994e+1	4.806e+1	1.519e+2	6.708e+1
f_8	F_w	7.215e+3	5.099e+3	1.001e-0	3.646e-4
	F_b	1.981e+3	2.714e+3	6.083e-3	3.826e-4
	F_{av}	6.721e+3	3.687e+3	1.326e-1	3.850e-4
f_9	F_w	2.901e-0	1.604e-0	9.030e-1	4.998e-1
	F_b	1.200e-0	1.007e-0	6.122e-1	3.998e-1
	F_{av}	1.749e-0	1.268e-0	7.508e-1	4.304e-1

superior convergent speed and accuracy, which the search capability is more suitable for the high dimension complex parameter identification problem than other algorithms.

IV. THE SLIDING MODE CONTROLLER AND PARAMETER OPTIMIZATION

The sliding mode control method is regarded as a variable structure systems, in which the sliding modes are induced by disruptive control forces. It has been studied extensively and successfully adopted in complex nonlinear systems owing to outstanding robustness against disturbances.

A. THE DESIGNING OF SLIDING MODE CONTROLLER (SMC)

Without loss of generality, considering the following nonlinear dynamic systems

$$\dot{x} = f(x,t) + g(x,t)u + d(t) \tag{25}$$

Here, f and g represent the nonlinear functions of the dynamic systems; $x = [x, \dot{x}, \cdots, x^{(n)}]^T$ denote the system tate variables; u represents the input force; $d(t)$ denotes uncertain disturbance.

Here, we denote the x_d as the reference position, the corresponding error between the reference point and system states is depicted as follows.

$$e(t) = x_d(t) - x(t) \tag{26}$$

Let sliding surface $s(e) = 0$, and sliding surface can be defined as follows.

$$s(e) = Ce \tag{27}$$

where $C = [c_1, c_2, \cdots, c_{n-1}, 1]$. According to the sliding mode control theory, the control law must force error vector $e(t)$ close to the sliding surface and move along with the sliding surface to the origin. Then, the control process can be divide into the approaching phase (letting $s(e) \neq 0$) and the sliding phase (letting $s(e) = 0$). For the approaching phase, the control law must satisfy the following condition $s(e)\dot{s}(e) < 0$ to drive the error e toward the sliding surface.

According to the aforementioned approaching phase condition, here, we denote the switching control law u_{sw} as follows.

$$u_{sw} = u_0 sgn\Big(s(e)\Big) \tag{28}$$

where $sgn()$ is the sign function, u_0 is unknown constant.

In the sliding phase, we denote the equivalent control u_{eq} as follows so as to propel the system dynamics to stay on the sliding surface. And the equivalent control force u_{eq} is acquired by letting $\dot{s}(e) = 0$.

$$\begin{aligned} \dot{s} &= C\dot{e} \\ &= C\frac{\partial s}{\partial x}(\dot{x}_d - \dot{x}) \\ &= C\left(\frac{\partial s}{\partial x}(\dot{x}_d) - \frac{\partial s}{\partial x}\Big(f(x,t) + g(x,t)u + d(t)\Big)\right) \\ &= 0 \end{aligned} \tag{29}$$

Here, to assume $\frac{\partial s}{\partial x}g(x,t)$ is non-singular. Then

$$u_{eq} = \left(\frac{\partial s}{\partial x}g(x,t)\right)^{-1}\left(\frac{\partial s}{\partial x}(\dot{x}_d) - \frac{\partial s}{\partial x}\Big(f(x,t) + d(t)\Big)\right) \tag{30}$$

The corresponding control law is obtained as follows.

$$u = u_{sw} + u_{eq} \tag{31}$$

$$\begin{aligned} &= u_0 sgn\Big(s(e)\Big) + \left(\frac{\partial s}{\partial x}g(x,t)\right)^{-1} \\ &\quad * \left(\frac{\partial s}{\partial x}(\dot{x}_d) - \frac{\partial s}{\partial x}\Big(f(x,t) + d(t)\Big)\right) \end{aligned} \tag{32}$$

B. PARAMETER OPTIMIZATION OF SMC

For implementing the parameter optimization, the parameters of SMC need to be encoded by decimal firstly. According to the overhead crane systems feature, the amplitude and residual oscillation of payload should keep as small as possible so as to avoid the unexpected accident, and trolley should move smoothly so as to rapidly and accurately arrival the appointed position. The cost function can be denoted as follows.

$$F_{cost} = \int_0^t |x|dt + 2 * \int_0^t |\theta|dt \tag{33}$$

where x and θ respectively denote trolley displacement and payload swing angle.

The optimization procedure is summarized as follows.

Step 1: Set up the parameter range of sliding mode controller;

Step 2: Initialize dynamic DE algorithm parameter such as $G = 500$, NP$= 30$, $p_c = 0.5$, $F_m^{ini} = 1.2$, $a = 50$, $b = 450$;

Step 3: Randomly generate NP groups sliding mode control parameter;

Step 4: Implement overhead crane systems control process for every group parameter and calculate the cost function value;

Step 5: Let $t = t + 1$ and $i = 1$;

Step 6: Calculate the dynamic scaling factor F_{dm} based on the eq.(22) and implement the mutation operation (eq.(21)) to acquire mutant individual v_i;

Step 7: According to the eq.(23), carry out the crossover operation between x_i and v_i to acquire new individual u_i;

Step 8: Let $i = i + 1$ and go to step 5 until $i = NP$;

Step 9: Perform overhead crane systems control process based on the new NP groups parameter and compute the cost function value;

Step 10: Implement selection operation to pick out the best NP groups parameter;

Step 11: Determine whether the best group parameter meets the iteration end condition. If it is met, then stop. Otherwise return to step 5.

V. SIMULATION EXPERIMENT OF OVERHEAD CRANE SYSTEMS

Based on the description of overhead crane systems, the overhead crane systems can be divided into trolley position subsystem and payload angle subsystem. The position sliding function and angle sliding function respectively are given as follows.

$$s_1(x_1, x_2) = c_1 x_1 + x_2 \tag{34}$$

$$s_2(x_3, x_4) = c_2 x_3 + x_4 \tag{35}$$

Then, the overall sliding function can be derived as:

$$\begin{aligned} s(x_1, x_2, x_3, x_4) &= \lambda_1 s_1 + \lambda_2 s_2 \\ &= \lambda_1 c_1 x_1 + \lambda_1 x2 + \lambda_2 c_2 x_3 + \lambda_2 x4 \end{aligned} \tag{36}$$

where $\lambda_1, \lambda_2, c_1, c_2$ are denoted as adjusted parameter of sliding function.

In order to verify the validity of the proposed method, the PID controller [4], optimized PID controller, sliding mode controller and optimized SMC are investigated and compared each other respectively. Without loss generality, these control methods are simulated under the following conditions.

Condition 1: payload weight $m = 1kg$, destination $x_d = 3$, $x_d = 7$.

Condition 2: payload weight $m = 3kg$, destination $x_d = 3$, $x_d = 7$.

Condition 3: payload weight $m = 9kg$, destination $x_d = 3$, $x_d = 7$.

The Fig.2, Fig.3 and Fig.4 respectively illustrate the results of trolley position and swing angle with different appointed position of three conditions. The corresponding parameters are listed in Table 2. In trolley position control aspect, the simulated control methods are enable to arrive at the appointed position accurately. Obviously, the PID control, optimized PID and optimized SMC drive the trolley to the destination more rapidly than unoptimized SMC. Note that, comparing with other three methods, the optimized SMC doesn't need too much adjustments when the trolley arrived at the appointed position.

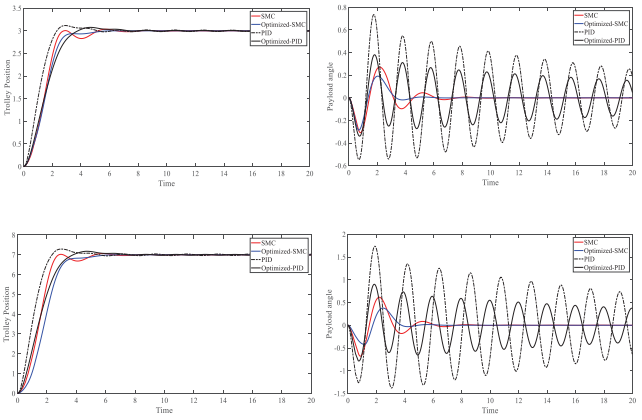

FIGURE 2. The position and angle simulation results under the first condition.

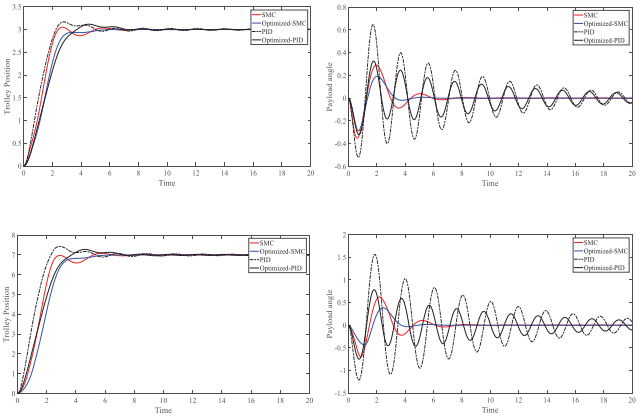

FIGURE 3. The position and angle simulation results under the second condition.

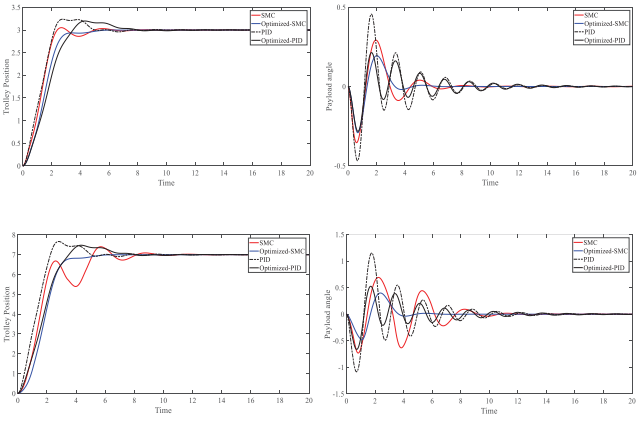

FIGURE 4. The position and angle simulation results under the third condition.

TABLE 4. The parameters of PID and SMC controllers.

PID	$K_p = 60$	$K_i = 0$	$K_d = 60$	$k = 0.8$	–
Optimized PID	$K_p = 31$	$K_i = 0$	$K_d = 46$	$k = 0.8$	–
SMC	$c_1 = 0.9$	$c_2 = 5$	$\lambda_1 = 1$	$\lambda_2 = -0.6$	$u_{eq} = 200$
Optimized SMC	$c_1 = 0.79$	$c_2 = 9.67$	$\lambda_1 = 1$	$\lambda_2 = -0.36$	$u_{eq} = 100$

In payload angle control aspect, the PID controllers (unoptimized and optimized) exhibit unsatisfied performance in eliminating residual vibration. In addition, the oscillation amplitude of the unoptimized PID controller is much higher than SMCs, which the maximum amplitude is close to 1.8 radian for the first condition. From the results we can infer that the anti-sway control performance of the PID controllers have highly correlated with payload weight and appointed point. It means that the eliminating residual vibration is relative good when payload is heavy and the amplitude is relative low when the specify point is not far, vice versa. The main reason is that itself linear characteristic of the PID controller cannot handle the nonlinear system effectively. In contrast, the SMCs can damp the payload residual vibration effectively with short time. Besides, the performance of amplitude is much better than PID controllers. And the payload weight has not too much effect on anti-swing performance. Most important, the optimized SMC gives the best anti-swing performance in eliminating residual vibration and damping the oscillation amplitude, which it can avoid the unexpected accident effectively.

VI. CONCLUSIONS

For eliminating the payload residual vibration, we firstly design a sliding mode controller for under-actuated overhead crane systems. Moreover, for configuring the SMC parameter efficiently, we propose a dynamic DE algorithm by introducing a dynamic scaling factor which is inspired by genetic scheme and utilize it to configure SMC parameters for solving the chattering problem. By simulating under three different operation conditions, the dynamic DE algorithm based SMC exhibits the best control performance in the trolley position and payload anti-swing control performance.

REFERENCES

[1] W. Singhose, L. Porter, M. Kenison, and E. Kriikku, "Effects of hoisting on the input shaping control of gantry cranes," *Control Eng. Pract.*, vol. 8, no. 10, pp. 1159–1165, 2000.

[2] K. L. Sorensen and W. E. Singhose, "Command-induced vibration analysis using input shaping principles," *Automatica*, vol. 44, no. 9, pp. 2392–2397, 2008.

[3] Y. Yoshida and H. Tabata, "Visual feedback control of an overhead crane and its combination with time-optimal control," in *Proc. IEEE/ASME Int. Conf. Adv. Intell. Mechatron.*, Jul. 2008, pp. 1114–1119.

[4] Z. Sun, N. Wang, Y. Bi, and J. Zhao, "A DE based PID controller for two dimensional overhead crane," in *Proc. 34th Chin. Control Conf. (CCC)*, Jul. 2015, pp. 2546–2550.

[5] H. Sano, K. Sato, K. Ohishi, and T. Miyazaki, "Robust design of vibration suppression control system for crane using sway angle observer considering friction disturbance," *Electr. Eng. Jpn.*, vol. 184, no. 3, pp. 36–46, 2013.

[6] N. Sun and Y. Fang, "Nonlinear tracking control of underactuated cranes with load transferring and lowering: Theory and experimentation," *Automatica*, vol. 50, no. 9, pp. 2350–2357, 2014.

[7] N. Sun, Y. Fang, H. Chen, and B. Lu, "Amplitude-saturated nonlinear output feedback antiswing control for underactuated cranes with double-pendulum cargo dynamics," *IEEE Trans. Ind. Electron.*, vol. 64, no. 3, pp. 2135–2146, Mar. 2017.

[8] N. Sun, Y. Fang, H. Chen, and B. He, "Adaptive nonlinear crane control with load hoisting/lowering and unknown parameters: Design and experiments," *IEEE/ASME Trans. Mechatronics*, vol. 20, no. 5, pp. 2107–2119, Oct. 2015.

[9] Y. Wu, R. Lu, P. Shi, H. Su, and Z.-G. Wu, "Analysis and design of synchronization for heterogeneous network," *IEEE Trans. Cybern.*, vol. 48, no. 4, pp. 1253–1262, Apr. 2018.

[10] Q. H. Ngo and K. S. Hong, "Sliding-mode antisway control of an offshore container crane," *IEEE/ASME Trans. Mechtronics*, vol. 17, no. 2, pp. 201–209, Apr. 2012.

[11] A. T. Le, S.-C. Moon, W. G. Lee, and S.-G. Lee, "Adaptive sliding mode control of overhead cranes with varying cable length," *J. Mech. Sci. Technol.*, vol. 27, no. 3, pp. 885–893, 2013.

[12] R. Liu and S. Li, "Suboptimal integral sliding mode controller design for a class of affine systems," *J. Optim. Theory Appl.*, vol. 161, no. 3, pp. 877–904, 2014.

[13] T. A. Le, S.-G. Lee, and S.-C. Moon, "Partial feedback linearization and sliding mode techniques for 2d crane control," *Trans. Inst. Meas. Control*, vol. 36, no. 1, pp. 78–87, 2014.

[14] M. S. Park, D. Chwa, and M. Eom, "Adaptive sliding-mode antisway control of uncertain overhead cranes with high-speed hoisting motion," *IEEE Trans. Fuzzy Syst.*, vol. 22, no. 5, pp. 1262–1271, Oct. 2014.

[15] S. Pezeshki, M. A. Badamchizadeh, A. R. Ghiasi, and S. Ghaemi, "Control of overhead crane system using adaptive model-free and adaptive fuzzy sliding mode controllers," *J. Control Autom. Electr. Syst.*, vol. 26, no. 1, pp. 1–15, 2015.

[16] M. Khazaee, A. H. D. Markazi, and E. Omidi, "Adaptive fuzzy predictive sliding control of uncertain nonlinear systems with bound-known input delay," *ISA Trans.*, vol. 59, pp. 314–324, Nov. 2015.

[17] D. Chwa, "Sliding-mode-control-based robust finite-time antisway tracking control of 3-D overhead cranes," *IEEE Trans. Ind. Electron.*, vol. 64, no. 8, pp. 6775–6784, Aug. 2017.

[18] K.-H. Cheng, "Adaptive B-spline-based fuzzy sliding-mode control for an auto-warehousing crane system," *Appl. Soft Comput.*, vol. 48, pp. 476–490, Nov. 2016.

[19] C. Du *et al.*, "A novel asynchronous control for artificial delayed Markovian jump systems via output feedback sliding mode approach," *IEEE Trans. Syst., Man, Cybern., Syst.*, to be published.

[20] S. Das, A. Mandal, and R. Mukherjee, "An adaptive differential evolution algorithm for global optimization in dynamic environments," *IEEE Trans. Cybern.*, vol. 44, no. 6, pp. 966–978, Jun. 2014.

[21] Q. Fan and X. Yan, "Self-adaptive differential evolution algorithm with zoning evolution of control parameters and adaptive mutation strategies," *IEEE Trans. Cybern.*, vol. 46, no. 1, pp. 219–232, Jan. 2016.

[22] R. A. Sarker, S. M. Elsayed, and T. Ray, "Differential evolution with dynamic parameters selection for optimization problems," *IEEE Trans. Evol. Comput.*, vol. 18, no. 5, pp. 689–707, Oct. 2014.

[23] Z. Sun, N. Wang, D. Srinivasan, and Y. Bi, "Optimal tunning of type-2 fuzzy logic power system stabilizer based on differential evolution algorithm," *Int. J. Elect. Power Energy Syst.*, vol. 62, no. 11, pp. 19–28, 2014.

[24] D. T. T. Do, S. Lee, and J. Lee, "A modified differential evolution algorithm for tensegrity structures," *Compos. Struct.*, vol. 158, pp. 11–19, Dec. 2016.

[25] C. Fu, C. Jiang, G. S. Chen, and Q. M. Liu, "An adaptive differential evolution algorithm with an aging leader and challengers mechanism," *Appl. Soft Comput.*, vol. 57, pp. 60–73, Aug. 2017.

[26] S. Suganthi, D. Devaraj, K. Ramar, and S. H. Thilagar, "An improved differential evolution algorithm for congestion management in the presence of wind turbine generators," *Renew. Sustain.Energy Rev.*, vol. 81, no. 1, pp. 635–642, 2018.
[27] L. Cui *et al.*, "Adaptive multiple-elites-guided composite differential evolution algorithm with a shift mechanism," *Inf. Sci.*, vol. 422, pp. 122–143, Jan. 2018.
[28] Z. Sun, N. Wang, Y. Bi, and D. Srinivasan, "Parameter identification of PEMFC model based on hybrid adaptive differential evolution algorithm," *Energy*, vol. 90, pp. 1334–1341, Oct. 2015.

ZHE SUN received the Ph.D. degree from Zhejiang University in 2015. He is currently with the Nanjing University of Posts and Telecommunications. His research interests include evolution computation, differential evolution algorithm, type-2 fuzzy logic system, and neural network.

XUEJIAN ZHAO received the Ph.D. degree from the Nanjing University of Aeronautics and Astronautics, Nanjing, China, in 2013. He is currently with the Nanjing University of Posts and Telecommunications. His research interests include Internet of Things, wireless sensor networks, and game theory.

ZHIXIN SUN received the D.E. degree from the Nanjing University of Aeronautics and Astronautics in 1998. He was a Post-Doctoral Researcher with Seoul National University from 2001 to 2002. He is currently a Professor with the Nanjing University of Posts and Telecommunications. His research interests include Internet computing and network security and the application of the Internet of Things.

FENG XIANG received the B.E. degree from Nanjing University. He is currently a Vice President with Yuantong Express Co., Ltd. His research interests include logistics engineering and business management.

CHUNJING MAO is currently a Vice President with Yuantong Express Co., Ltd. His research interests include computer network and logistics engineering.